Analysis of MQW and Anisotropic Guided Wave Structures Using a Full-Wave 2D TLM-Based FD-TD Method

Zhizhang Chen*, **Man Leung Lui***, **Pierre Berini**+ and **Ke Wu**++
*Department of Electrical and Computer Engineering, Dalhousie University
Halifax, Nova Scotia, Canada B3J 2X4
+Department of Electrical Engineering, University of Ottawa, Ottawa, Ontario K1N 6N5
++Ecole Polytechnique de Montreal, Montreal, Quebec, Canada H3C 3A7

Abstract-A 2D full-wave TLM (transmission-line-matrix) technique was reported before for the analysis of arbitrarily shaped guided wave structures. However, the computations involve the operations on the third spatial step Δz. In this paper, another 2D full-wave TLM-based method is presented where no third spatial dimension operations are required at all. The method is derived by assuming the field variation of $e^{-j\beta z}$ along the z-direction (the propagation direction) in the 3D TLM based finite-difference time-domain (FD-TD) method. As a result, a truly two-dimensional scheme is developed with both electric and magnetic components condensed at every numerical grid point. The method was applied to a microstrip line deposited on an anisotropic substrate and a multiple quantum well (MQW) structure where the dielectric constant of the MQW substrate varies with spatial positions. The numerical results agree well with the results obtained from other techniques, and therefore validate the effectiveness of the 2D technique based on the TLM principle.

I. INTRODUCTION

Two widely employed time-domain techniques for modelling electromagnetic structures are the finite-difference time-domain (FD-TD) method and the transmission-line-matrix (TLM) method proposed. To exploit the features of both FD-TD and TLM, an FD-TD formulation based on the TLM scheme was proposed in [3] for a uniform mesh, and a further demonstration in a more general case was shown in [2]. The progress in implementation of various modelling schemes in this TLM based technique, such as the Perfectly Matched Layer (PML) and nonlinearity, were presented in [3].

To improve the computation efficiency for the analysis of guided wave structures, a full-wave two-dimensional TLM scheme was developed in [4]. In the method, $e^{-j\beta \Delta z}$ is introduced to account for the wave propagation along the z-direction. The resultant formulations are dependent on Δz. A further improved technique which removes any involvement of Δz was made but was demonstrated only on the Yee's FD-TD grid [5][6][7]. On the other hand, to the authors' best knowledge, this improved 2D technique has not been applied to the TLM based method. The reason is probably that the TLM scheme is formulated in terms of impulse scattering at nodes (which are connected by a network of transmission lines) rather than an explicit expression of Maxwell's equations.

In this paper, we report the successful adaption of the improved 2D full-wave scheme to the TLM based technique in the form of TLM based FD-TD formulation, leading to another full-wave 2D TLM-based method.

II. THE FULL-WAVE 2D TLM BASED FD-TD FORMULATIONS

The full-wave 2D TLM based FD-TD technique is derived from the 3D TLM based FD-TD formulations. Therefore, we start with the 3D TLM based FD-TD formulations.

0-7803-4471-5/98/$10.00 (c) 1998 IEEE

A. The 3D TLM-Based FD-TD Formulas

In a 3D TLM-based FD-TD cell with dimensions $\delta x \times \delta y \times \delta z\,(=u\Delta l \times v\Delta l \times w\Delta l)$, all six field components of $\boldsymbol{E}$, $\boldsymbol{H}$ and their corresponding flux densities, $\boldsymbol{D}$ and $\boldsymbol{B}$, are defined at the center, while at the grid points on the boundary surfaces of the cell, only the field components tangential to the surfaces are considered [3][2].

By simply finite-differencing Maxwell's equations with respect to the center of a 3D cell, finite difference formulations can be easily obtained for the field components at the center of a 3D cell. For example, for the D_x component, we obtain:

$$
\begin{aligned}
&[\tfrac{vw}{u}\ \tfrac{uD_x^n(i,j,k)}{\varepsilon_o} + g_x\, uE_x^n(i,j,k)] \\
&= \tfrac{vw}{u}\ \tfrac{uD_x^{n-1}(i,j,k)}{\varepsilon_o} - g_x\, uE_x^{n-1}(i,j,k) \\
&- \tfrac{1}{s}[vZ_oH_y^{n-\frac{1}{2}}(i,j,k+\tfrac{1}{2}) - vZ_oH_y^{n-\frac{1}{2}}(i,j,k-\tfrac{1}{2})] \\
&+ \tfrac{1}{s}[wZ_oH_z^{n-\frac{1}{2}}(i,j+\tfrac{1}{2},k) - wZ_oH_z^{n-\frac{1}{2}}(i,j-\tfrac{1}{2},k)]
\end{aligned}
\tag{1}
$$

where $g_x = \frac{vw}{u}\ \frac{\sigma_{ex}\delta t}{\varepsilon_o}$, $r_y = \frac{uw}{v}\ \frac{\sigma_{mx}\delta t}{\mu_o}$, and stability factor $s = \frac{\Delta l/c}{\delta t}$.

The E and H field components at the center of a cell are found through a solution of the medium constitutive relationship: **D=D(E,H)** and **B=B(E,H)**.

The field components at the boundary surfaces of the cell can be updated through a special averaging process in both space and time. For instance, we have:

$$
\begin{aligned}
&uE_x^{n+\frac{1}{2}}(i,j,k+\tfrac{1}{2}) \\
&= -0.5[uE_x^{n-\frac{1}{2}}(i,j,k-\tfrac{1}{2}) + q_{xy}\, vZ_oH_y^{n-\frac{1}{2}}(i,j,k-\tfrac{1}{2})] \\
&- 0.5[uE_x^{n-\frac{1}{2}}(i,j,k+\tfrac{3}{2}) - q_{xy}\, vZ_oH_y^{n-\frac{1}{2}}(i,j,k+\tfrac{3}{2})] \\
&+ [uE_x^n(i,j,k) + q_{xy}\, vZ_oH_y^n(i,j,k)] + [uE_x^n(i,j,k+1) \\
&- q_{xy}\, vZ_oH_y^n(i,j,k+1)]
\end{aligned}
\tag{2}
$$

Here $Z_o = \sqrt{\frac{\mu_o}{\varepsilon_o}}$. q_{xy} is a constant which determines the type of the TLM node to which the proposed FD-TD is equivalent. For instance, selecting q_{xy}=1 will make the TLM based FD-TD equivalent to the TLM Symmetrical Condensed Node while using $q_{xy} = \frac{\mu_y uw}{v}$ will make the FD-TD equivalent to the TLM Hybrid Symmetrical Condensed Node.

B. The 2D Full-Wave TLM-Based FD-TD Formulas

By applying the similar procedure as described in [7], we assume that

$$
[D_x, D_y, B_z] = [D_x(x,y), D_y(x,y), B_z(x,y)]\, j\, e^{-j\beta z} \tag{3}
$$

$$
[B_x, B_y, D_z] = [B_x(x,y), B_y(x,y), B_z(x,y)]\, e^{-j\beta z} \tag{4}
$$

$$
[E_x, E_y, H_z] = [E_x(x,y), E_y(x,y), H_z(x,y)]\, j\, e^{-j\beta z} \tag{5}
$$

$$
[H_x, H_y, E_z] = [H_x(x,y), H_y(x,y), E_z(x,y)]\, e^{-j\beta z} \tag{6}
$$

(1) and (2) then become:

$$
\begin{aligned}
&[\tfrac{vw}{u}\ \tfrac{uD_x^n(i,j)}{\varepsilon_o} + g_x\, uE_x^n(i,j)] = \\
&\tfrac{vw}{u}\ \tfrac{uD_x^{n-1}(i,j)}{\varepsilon_o} - g_x uE_x^{n-1}(i,j) \\
&- \beta c\, \delta t\, vZ_oH_y^{n-\frac{1}{2}}(i,j) \\
&+ \tfrac{1}{s}[wZ_oH_z^{n-\frac{1}{2}}(i,j+\tfrac{1}{2}) - wZ_oH_z^{n-\frac{1}{2}}(i,j-\tfrac{1}{2})]
\end{aligned}
\tag{7}
$$

$$
uE_x^{n+\frac{1}{2}}(i,j) = 2\, uE_x^n(i,j) - uE_x^{n-\frac{1}{2}}(i,j) \tag{8}
$$

The third dimension discretization Δz is now completely removed and the index k disappears. The equations for the other components can be obtained in a similar way.

Fig. 1 shows the grid arrangement for the 2D TLM based FD-TD scheme. As expected, all of the field components are defined at the center of a 2D cell while on the boundary surfaces, only the tangential field components are defined. This is different from the grid arrangement based on the Yee's grid as shown in [7].

0-7803-4471-5/98/$10.00 (c) 1998 IEEE

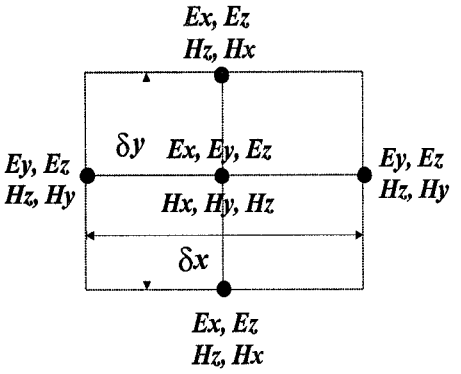

Fig.1 Grid arrangement of the 2D TLM based FD-TD method

III. NUMERICAL RESULTS

Two examples were computed. One is the open microstrip line deposited on an electrically and magnetically anisotropic substrate [8] and the second one is the InGaAs/GaAs MQW field-induced optical waveguide as described in [9].

In the first example, the geometry and parameters of the microstrip line were taken to be the same as those used in [8] with

$$\varepsilon_{11} = \varepsilon_{x1}cos^2\theta + \varepsilon_{z1}sin^2\theta, \quad \varepsilon_{33} = \varepsilon_{x1}sin^2\theta + \varepsilon_{z1}cos^2\theta,$$
$$\varepsilon_{22} = \varepsilon_{y1}, \quad j\varepsilon_{13} = -j\varepsilon_{31} = (\varepsilon_{z1} - \varepsilon_{x1})\,sin\theta cos\theta,$$
$$\mu_{11} = \mu_{x2}cos^2(\theta+\Delta\theta) + \mu_{z2}sin^2(\theta+\Delta\theta),$$
$$\mu_{33} = \mu_{x2}sin^2(\theta+\Delta\theta) + \mu_{z2}cos^2(\theta+\Delta\theta), \quad \mu_{22} = \mu_{y2}, \text{ and}$$
$$j\mu_{13} = -j\mu_{31} = (\mu_{z2} - \mu_{x2})\,sin(\theta+\Delta\theta)cos(\theta+\Delta\theta).$$

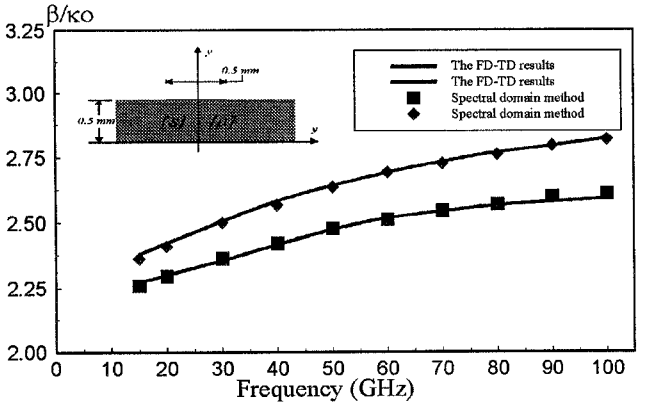

Fig. 2 Calculated dispersion of the anisotropic microstrip line

Note that $\pm j$ is introduced because of the coupling between transverse and longitudinal components as the result of nonzero ε_{13}, ε_{13}, μ_{13}, and μ_{31} [10].

Two cases were computed: (1) θ=0, $\Delta\theta$=0 and (2) θ=15^o, $\Delta\theta$=58^o. The results are found to be in a very good agreement with those obtained using the spectrum domain technique [8] (see Fig. 2).

In the second example, the GaAs-based optical waveguide structure consisting of AlGaAs/GaAs top/bottom cladding layers and an embedded InGaAs/GaAs MQW core is considered [9] (see Fig. 3). The operation of the device depends on a field-induced increase in refractive index within the MQW core as a function the negative bias applied to the electrode. The change of the refractive index in the MQW is shown in Fig. 3. Because the media are simple and anisotropic, the 2D FD-TD computations involve only real-number calculations.

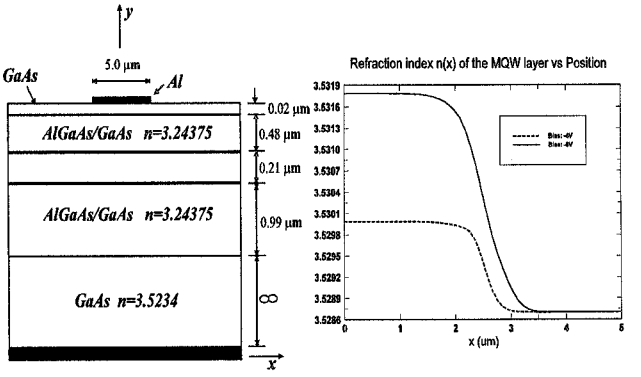

Fig.3 Geometry of the MQW structure

The propagation constants were computed and are shown in Table I. They are in good agreement with the results obtained with the method of line (MoL) [9]. In our computations, a 30×31 nonuniform grid was used. The aluminum electrode was not considered. The difficulty in modelling the aluminum electrode arises from the fact that the aluminum presents a

negative real permittivity at optical frequencies. This negative permittivity can cause instabilities in the FD-TD scheme. Fortunately, most of the energy is concentrated in the MQW layer and the electrode has little effects on the propagation constant as indicated in [9].

Table I

Computed normalized propagation constant β/β_o for the MQW structure

Mode	Bias (V)	*MoL*	*this method*	Diff. (%)
E_x^{11}	-8	3.368974	3.393638	0.72
E_y^{11}	-8	3.353880	3.387479	1.00
E_x^{11}	-4	3.367963	3.381950	0.42
E_y^{11}	-4	3.353030	3.385097	0.96

V. CONCLUSIONS

In this paper, a full-wave two-dimensional TLM based technique is developed for the analysis of arbitrarily shaped guided wave structures. Unlike the previously developed 2D TLM full-wave scheme, the method presented here involves no operations on the third spatial step Δz. In addition, both electric and magnetic fields are defined at numerical grid points.

In conclusions, the 2D TLM-based FD-TD offers another efficient TLM based CAD tool for the practical computer-aided design of various RF, microwave and optical circuits.

REFERENCES

[1] Z. Chen, M. M. Ney and W. J. R. Hoefer, ``A new finite-difference time-domain formulation and its equivalence with the TLM symmetrical condensed node", *IEEE Trans. Microwave Theory Tech.* , Vol. 39, No. 12, pp. 2160 – 2169, Dec. 1991

[2] Z. Chen, ``The generalized TLM based finite-difference time-domain method and its applications to frequency-dependent and anisotropic media", *Digest of 1996 IEEE International Microwave Symposium,* San Francisico, June 17-21, 1996

[3] Z. Chen and J. Xu, ``The TLM based FD-TD--Summary of recent progress", *IEEE Microwave and Guided Wave Letters,* Vol. 7, No. 1, pp. 12-14, Jan., 1997

[4] J. Hang and R. Vahldieck, ``Full-wave analysis of guiding structures using a 2D-array of 3D TLM nodes", *IEEE Trans. Microwave Theory Tech.* , Vol. 41, No. 3, pp. 472 – 477, March 1993

[5] S. Xiao, R. Vahldieck and H. Jin, ``Full-wave analysis of guided wave structures using a novel 2D FDTD", *IEEE Microwave and Guided Wave Letters,* Vol. 2, No. 5, pp. 165-167, May, 1992

[6] A. Si and L. Shafai, ``Dispersion analysis of anisotropic imhomogeneous waveguides using compact 2-D FDTD", *Electronics Letters.,* Vol. 28, No. 15, pp. 1151-1152, July 1992

[7] S. Xiao and R. Vahldieck, ``An efficient 2D FDTD algorithm using real variables", *IEEE Microwave and Guided Wave Letters,* Vol. 3, No. 5, pp. 127-129, May, 1993

[8] Y. Chen and B. Beker, ``Dispersion characteristics of open and shielded microstrip lines under a combined principal axes rotation of electrically and magnetically anisotropic substrates", *IEEE Trans. Microwave Theo. Tech.,* Vol. 41, No. 4, pp. 673-679, April, 1993

[9] P. Berini, A. Stohr, K. Wu and D. Jager, "Normal mode analysis and characterization of an InGaAs/GaAs MQW field-induced optical waveguide including electrode effects," *Journal of Lightwave Technology*, vol. 14, No. 10, pp.2422-2435, 1996.

[10] A. Zhao, J. Juntunen, and A. Raisanen, ``Relationship between the compact complex and real variable 2-D FDTD methods in arbitrary anisotropic dielectric waveguides", *Digest of 1997 IEEE International Microwave Symposium,* Denver, June 8-13-21, pp. 83-86, 1997